Reduced-Order Model for the Catalytic Cracking of Bio-Oil

Francisco José de Souza * , Jonathan Utzig , Guilherme do Nascimento , Alicia Carvalho Ribeiro , Higor de Bitencourt Rodrigues , Henry França Meier

Posted Date: 11 June 2025

doi: 10.20944/preprints202506.0674.v1

Keywords: bio-oil; fluid catalytic cracking; FCC riser; reduced-order model

Article

Reduced-Order Model for the Catalytic Cracking of Bio-Oil

Francisco José de Souza [1,*,†,‡], Jonathan Utzig [2,‡], Guilherme do Nascimento [2,‡], Alicia Carvalho Ribeiro [2,‡], Higor de Bitencourt Rodrigues [2,‡] and Henry França Meier [2,‡]

[1] Federal University of Uberlandia
[2] Regional University of Blumenau
* Correspondence: francisco.souza@ufu.br
† Current address: School of Mechanical Engineering. Av Joao Naves de Avila 2121, Uberlândia - MG - Brazil
‡ These authors contributed equally to this work.

Abstract: This work presents a one-dimensional (1D) model for simulating the behavior of an FCC riser reactor processing bio-oil. The FCC riser is modeled as a plug-flow reactor, where the bio-oil feed undergoes vaporization followed by catalytic cracking reactions. The bio-oil droplets are represented using a Lagrangian framework, which accounts for their movement and evaporation within the gas-solid flow field, enabling the assessment of droplet size impact on reactor performance. The cracking reactions are modeled using a four-lumped kinetic scheme, representing the conversion of bio-oil into gasoline, kerosene, gas plus coke. The simulation results are validated against experimental data from a full-scale FCC unit, demonstrating good agreement in terms of product yields. The findings indicate that heat exchange by radiation is negligible and that the Buchanan correlation best represents the heat transfer between the droplets and the catalyst particles/gas phase. Another significant observation is that droplet size, across a wide range, does not significantly affect conversion rates due to the bio-oil's high vaporization heat. The proposed reduced-order model provides valuable insights into optimizing FCC riser reactors for bio-oil processing while avoiding the high computational costs of 3D CFD simulations.

Keywords: bio-oil; fluid catalytic cracking; FCC riser; reduced-order model

1. Introduction

The increasing demand for sustainable energy sources has driven significant research into the utilization of bio-oil in fluid catalytic cracking (FCC) reactors. Bio-oil, derived from biomass, presents a promising alternative to conventional fossil fuels due to its renewable nature and potential for reducing greenhouse gas emissions. Pilot-scale experimental tests have proven the feasibility of co-processing raw or pyrolysis bio-oils and attested to the presence of renewable carbon in the processed fuels [1,2]. However, the complex chemical composition and behavior of bio-oil in FCC processes require advanced modeling techniques to optimize reactor performance and product yields.

Numerous numerical studies have investigated FCC risers operating with gas oil [3,4], while only a few have focused on bio-oil operations [5,6], primarily using Computational Fluid Dynamics (CFD) methods. Despite significant advances in computer hardware and software, two- and three-dimensional CFD models remain computationally demanding. Consequently, developing alternative models that provide faster results without considerable loss of accuracy is of practical importance.

Recent advances in computing hardware have significantly enhanced fluid flow simulation capabilities. However, complex multiphase flows, such as those in circulating fluidized beds, remain challenging due to dominant spatial structures and intricate variable interactions that are difficult to capture. The oil atomization, droplet-particle collision, and multicomponent evaporation are some of the many complex phenomena that take place inside the reactor. The complete mathematical

 doi:10.20944/preprints202506.0674.v1

description of such physical behavior is far to be accomplished. To support both design and control, accurate yet computationally efficient models are crucial.

A promising approach is the use of reduced-order models (ROMs), which extract dominant flow features and solve only for their corresponding weighting coefficients, thereby drastically reducing the number of degrees of freedom. Brenner *et al.* (2012) developed a ROM for non-isothermal flow based on full-order CFD simulations of a two-dimensional fluidized bed using a two-phase hydrodynamic model, demonstrating excellent agreement with high-fidelity results [7]. Huang *et al.* (2018) highlight the potential of mathematically rigorous ROMs for efficiently and accurately simulating combustion dynamics. While projection-based ROMs significantly lower computational costs, their accuracy depends on capturing sharp gradients in temperature and species concentrations, key characteristics of reacting flows [8].

In this study, we present a reduced-order model (ROM) for FCC reactors operating with bio-oil feedstock. The model builds upon the approach proposed by [9] and is implemented in MATLAB, leveraging its computational efficiency to perform complex analyses within seconds. This rapid processing capability facilitates extensive parametric studies and optimization tasks, which are essential for the practical application of bio-oil in FCC units.

The proposed model employs a one-dimensional Eulerian framework for the gas phase, ensuring a simplified, yet accurate, representation of the reactor's fluid dynamics. Simultaneously, catalyst particles and bio-oil droplets are treated using a Lagrangian approach, capturing their discrete nature and interactions with the gas flow. This hybrid modeling strategy enables a detailed analysis of multiphase flow behavior and reaction kinetics, offering valuable insights into FCC reactor performance and optimization for bio-oil processing.

The model's reduced-order nature, combined with its high computational efficiency, makes it a valuable tool for both academic research and industrial applications, particularly in the preliminary design and analysis of more sustainable and optimized FCC processes handling bio-oil. Validation against experimental data confirms its reliability, with results showing good agreement with the findings of [10]. These results underscore the potential of reduced-order modeling to accurately capture key flow characteristics while drastically reducing computational costs, providing a practical alternative to full CFD simulations for process analysis, optimization, and control. The model also facilitates the identification of challenges and issues associated with adapting existing FCC units for bio-oil processing. By providing rapid insights into fluid dynamics, reaction kinetics, and heat transfer, it helps pinpoint key operational limitations and optimization opportunities. These include factors such as steam, catalyst and feed flow rates, feedstock vaporization behavior, and potential modifications required to maintain efficiency. This capability makes the model a valuable tool for assessing feasibility and guiding practical adaptations in industrial FCC processes.

2. Mathematical Model

The simplified model used in this work is based on one-dimensional, steady-state conservation equations for the gas phase within an Eulerian framework. Catalyst particles and oil droplets are treated using a Lagrangian approach, modified to consider the axial direction of the riser. Specifically, the continuity and energy equations are solved for the gas phase, while the pressure gradient across the fluidized bed is determined by considering only the most relevant contributions, allowing gas movement. Regarding the droplets and particles, only drag, weight, and buoyancy effects are included. Additionally, heat exchange via convection and radiation between the gas and the particles, as well as between the gas and the droplets, is accounted for. Furthermore, heat transfer between the particles and droplets is incorporated into the mathematical model. Both droplets and particles are fed at the bottom of the riser and move upward through the reactor due to the drag of the gas phase.

 doi:10.20944/preprints202506.0674.v1

2.1. Transport Equations

Gas continuity

$$\frac{d(\epsilon_g \rho_g u_g)}{dx} = -N_d \dot{m}_{vap}, \tag{1}$$

where ϵ_g denotes the gas volume fraction, ρ_g is the gas density and u_g the gas velocity. On the RHS, Nd represents the droplet number density, i.e., the actual number of droplets per total volume, and $\dot{m}_{vap}$ is the droplet vaporization rate.

Gas energy

if $T_d < T_{bp}$ and $d_d > 0$

$$\frac{d(\epsilon_g \rho_g u_g C p_g T_g)}{dx} = h_{gs} A_s N_s (T_s - T_g) + h_{gd} A_d N_d (T_d - T_g) + \sigma k_B A_d N_d (T_d^4 - T_g^4) + \sigma k_B A_s N_s (T_s^4 - T_g^4), \tag{2}$$

if $T_d = T_{bp}$ and $d_d > 0$

$$\frac{d(\epsilon_g \rho_g u_g C p_g T_g)}{dx} = h_{gs} A_s N_s (T_s - T_g) + \sigma k_B A_s N_s (T_s^4 - T_g^4) + L_v N_d \dot{m}_{vap}, \tag{3}$$

where T_{bp} is the boiling point of the liquid, Cp_g is the heat capacity of the gas phase and T_g is the gas temperature, h_{gs} is the convective heat transfer coefficient between the gas and the particles, A_s is the surface area of the catalyst particle, N_s represents the particle number density, i.e., the actual number of particles per total volume, T_s is the particle temperature, h_{gd} is the convective heat transfer coefficient between the gas and the droplets, σ is the emissivity, k_B is the Stefan-Boltzmann constant and L_v denotes the latent heat of vaporization of the droplets.

Vaporizing species continuity

$$\frac{d(\epsilon_g u_g C_i)}{dx} = -\frac{N_d \dot{m}_{vap}}{MW_i} + R_i, \tag{4}$$

where C_i is the molar concentration of the vaporization species (gas oil or bio-oil) in the gas phase, MW_i its molecular weight and R_i, its reaction rate.

Other species continuity

$$\frac{d(\epsilon_g u_g C_i)}{dx} = R_i, \tag{5}$$

where C_i is the molar concentration of species i in the gas phase and R_i the total reaction rate.

Pressure gradient across riser

$$\frac{dP}{dx} = \epsilon_g \rho_g g + \epsilon_s \rho_s g - \frac{2 f_g \epsilon_g \rho_g u_g u_g}{D} - \frac{2 f_s \epsilon_s \rho_s u_s u_s}{D}, \tag{6}$$

where P is pressure, f_g and f_s are friction factors and D is the riser diameter.

Solid continuity

$$\frac{d(\epsilon_s \rho_s u_s)}{dx} = 0, \tag{7}$$

ϵ_s represents the solid volume fraction, ρ_s is the solid density and u_s is the solid velocity. Equation (7) is used to determine the gas volume fraction, ϵ_g, through the relation:

$$\epsilon_s + \epsilon_g = 1. \tag{8}$$

 doi:10.20944/preprints202506.0674.v1

Solid momentum

$$\frac{du_s}{dx} = 0.75\frac{C_D\rho_g|u_g - u_s|}{d_s\rho_s u_s}(u_g - u_s) + \frac{(\rho_g - \rho_s)}{\rho_s u_s}g, \tag{9}$$

where C_D is the drag coefficient, d_s the particle diameter and g is the gravity acceleration. To derive Equation (9), the following transformation was used:

$$dx = u_s dt. \tag{10}$$

Solid energy

$$\frac{d(\epsilon_s\rho_s u_s Cp_s T_s)}{dx} = h_{gs}A_s N_s(T_g - T_s) + \sigma k_B A_s N_s(T_g^4 - T_s^4) - Q_{reaction}, \tag{11}$$

Cp_s is the heat capacity of the particle, ρ_s is the solid density, T_s is the solid temperature and $Q_{reaction}$ is the heat of reaction due to the cracking reactions:

$$Q_{reaction} = \Sigma_i r_i \Delta H_{react,i}, \tag{12}$$

i runs over all reactions included in the kinetic mechanism, r_i is the i^{th} reaction rate and ΔH_i its respective enthalpy.

Droplet continuity

$$\frac{dm_d}{dx} = \frac{\dot{m}_{vap}}{u_d}, \tag{13}$$

with m_d representing the droplet mass and u_d the droplet velocity.

Droplet diameter

$$\frac{dd_d}{dx} = \frac{2\dot{m}_{vap}}{\pi\rho_d u_d d_d^2}. \tag{14}$$

Droplet momentum

$$\frac{du_d}{dx} = 0.75\frac{C_D\rho_g|u_g - u_d|}{d_d\rho_d u_d}(u_g - u_d) + \frac{(\rho_g - \rho_d)}{\rho_d u_d}g. \tag{15}$$

Droplet energy

if $T_d < T_{vap}$

$$\frac{dT_d}{dx} = \frac{h_{gd}A_d(T_g - T_d) + \sigma k_B A_d(T_g^4 - T_d^4)}{m_d u_d Cp_d}, \tag{16}$$

if $T_d >= T_{vap}$ and $T_d < T_{bp}$

$$\frac{dT_d}{dx} = \frac{h_{gd}A_d(T_g - T_d) + \sigma k_B A_d(T_g^4 - T_d^4) + L_v\dot{m}_{vap}}{m_d u_d Cp_d}, \tag{17}$$

if $T_d = T_{bp}$

$$\frac{dT_d}{dx} = 0, \tag{18}$$

Cp_d is the droplet heat capacity and T_{vap} is the vaporization temperature. To derive the droplet equations above, the following transformation was used:

$$dx = u_d dt. \tag{19}$$

2.1.1. Auxiliary Relations

Drag Coefficient [11]

 doi:10.20944/preprints202506.0674.v1

$$C_D = \begin{cases} \frac{24}{Re_s}(1 + 0.15Re_s^{0.687}), & \text{if } Re_s < 1000; \\ 0.44, & \text{otherwise,} \end{cases} \tag{20}$$

$$C_D = \begin{cases} \frac{24}{Re_d}(1 + 0.15Re_d^{0.687}), & \text{if } Re_d < 1000; \\ 0.44, & \text{otherwise,} \end{cases} \tag{21}$$

where Re_s and Re_d represent the particle and droplet Reynolds numbers, respectively:

$$Re_s = \frac{\rho_g d_s |u_g - u_s|}{\mu}, \tag{22}$$

$$Re_d = \frac{\rho_g d_d |u_g - u_d|}{\mu}, \tag{23}$$

and μ is the dynamic viscosity of the gas phase.

Gas density

$$\rho_g = \Sigma_i C_i MW_i, \tag{24}$$

where the summation runs over all the species in the gas phase (oil, steam, light gas, gasoline and kerosene).

Heat transfer coefficients

Gas-solid

$$Nu_{gs} = \frac{h_{gs} d_s}{k} = 2 + 0.6Re_s^{\frac{1}{2}} Pr^{\frac{1}{3}}, \tag{25}$$

where Pr is the Prandtl number:

$$Pr = \frac{Cp_g \mu}{k}. \tag{26}$$

Gas-droplet

Ranz-Marschall correlation

$$Nu_{gd} = \frac{h_{gd} d_d}{k} = 2 + 0.6Re_d^{\frac{1}{2}} Pr^{\frac{1}{3}}, \tag{27}$$

Buchanan correlation

$$Nu_{gd} = \frac{h_{gd} d_d}{k} = 2 + 0.6Re_{eff}^{\frac{1}{2}} Pr^{\frac{1}{3}}, \tag{28}$$

the effective Reynolds number Re_{eff} is defined as:

$$Re_{eff} = \frac{\rho_s \epsilon_s d_d |u_g - u_d|}{\mu}. \tag{29}$$

It is worth mentioning that the effective Reynolds number used by Buchanan's model considers the solid phase density ρ_s instead of the gaseous, resulting in a higher heat transfer between the phases.

Vaporization rate

if $T_{vap} < T_d < T_{bp}$:

$$\dot{m}_{vap} = -A_d N_{vap} MW, \tag{30}$$

in such temperature range, it is assumed that the mass transfer from the droplet to the surrounding gas is limited by convection. N_{vap} represents the gas oil or bio-oil vapor flux from the droplet surface to the gas phase and MW its respective molecular weight:

$$N_{vap} = k_c(C_s - C_i), \tag{31}$$

 doi:10.20944/preprints202506.0674.v1

k_c is the convective mass transfer coefficient, which can be calculated as follows:

$$Sh_{gd} = \frac{k_c d_d}{D_{eff}} = 2 + 0.6 Re_d^{\frac{1}{2}} Sc^{\frac{1}{3}}, \tag{32}$$

the Schmidt number Sc is given by:

$$Sc = \frac{\mu}{\rho_g D_{eff}}, \tag{33}$$

and D_{eff} is the effective diffusivity in the gas phase. C_s and C_i are the molar concentrations of the vaporizing species at the droplet-gas interface and in the bulk gas phase, respectively. Vapor-liquid equilibrium is assumed at the interface, with the saturation pressure given by:

$$P_{sat} = P.e^{\frac{L_v MW}{R}(\frac{1}{T_{bp}} - \frac{1}{T_d})}, \tag{34}$$

where P_{sat} is the saturation pressure at temperature T_d. C_s can be calculated as:

$$C_s = \frac{P_{sat}}{RT_d}. \tag{35}$$

If $T_d = T_{bp}$, i.e., during the boiling phase, the vaporization rate reads:

$$\dot{m}_{vap} = -\frac{h_{gd}(T_g - T_d)}{L_v} - \frac{\sigma k_B A_d N_d (T_g^4 - T_d^4)}{L_v}. \tag{36}$$

2.2. Reaction Mechanisms

2.2.1. Gas Oil Catalytic Cracking

All reaction rates are calculated as:

$$r_i = k_r (C_i)^n \phi. \tag{37}$$

The variation of the kinetic constant k_r with temperature is given by the Arrhenius equation:

$$k_r = k_r^0 e^{-\frac{E_a}{RT}}, \tag{38}$$

where k_r^0 is the pre-exponential factor, E_a is the activation energy. The parameter ϕ represents the catalyst activity, which can reduce due to coke deposition ([12]):

$$\phi = e^{-8633 \frac{C_{coke}}{\rho_s \epsilon_s}}. \tag{39}$$

For the gas oil, the 4-lumped scheme proposed by [12] is used (Figure 1), involving the following species: gas oil, gasoline, light gas and coke. Such simplified reaction mechanism has been shown to provide satisfactory results as demonstrated in previous works [3]. Essentially, the gas oil cracking reactions are modeled as 2^{nd} order reactions (n=2), while the gasoline cracking is modeled as 1^{st} order reactions (n=1). Table 1 presents the pre-exponential factors, activation energies and heat of reaction for this model.

Since [12] conducted the experiments at 550^oC it is necessary to correct the reaction constants at such temperature to arbitrary temperatures. Furthermore, they depend on the solid concentration. In order to make predictions at any temperature e catalyst concentration, the pre-exponential factor in the Arrhenius equation has been isolated and multiplied by the local solid concentration. Thus, the kinetic constants are recalculated as below:

$$k_r = k_{r,823K} e^{\frac{-E_a}{R}(\frac{1}{T_g} - \frac{1}{823.15})} \rho_s \epsilon_s. \tag{40}$$

 doi:10.20944/preprints202506.0674.v1

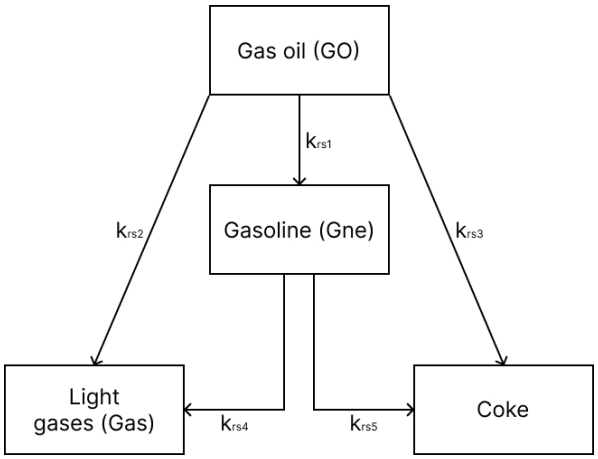

Figure 1. 4-lump gas oil reaction mechanism.

Table 1. Kinetic data for the 4-lumped gas oil cracking mechanism. Reaction constants are from [12] and the remaining data are from [13].

Reaction number	reactant/product	$k_{r,550^oC}$ $(m^6/(kg.kg_s.s))$ or $m^3/(kg_s.s))$	Activation Energy (kJ/kmol)	Heat of Reaction (kJ/kg)
1	GO → Gne	20.4	68,316	195
2	GO → Gas	7.8	89,303	670
3	GO → Coke	3	64,629	745
4	Gne → Gas	$1.33x10^{-4}$	52,769	530
5	Gne → Coke	$2.67x10^{-4}$	115,556	690

2.2.2. Bio-Oil Catalytic Cracking

Generally speaking, bio-oil is a multi-component mixture derived from biomass pyrolysis, consisting of oxygenated compounds such as phenols, furans, carboxylic acids, and ketones. Thus, simulating bio-oil catalytic cracking in an FCC riser model presents several challenges due to the complexity of bio-oil composition and reaction kinetics. Unlike conventional petroleum feedstocks, bio-oil has a wide molecular weight distribution and varying chemical reactivity, making it difficult to develop accurate kinetic models that capture the full spectrum of its cracking behavior.

The simulation of bio-oil catalytic cracking in an FCC riser reactor requires a representation of complex reaction kinetics, phase interactions, and thermal behaviors. While the fundamental computational approach has already been outlined, in this section the modifications required to simulate bio-oil conversion and the key parameters influencing reaction pathways and product yields are described.

To model the reactions, the simulation employs a lumped kinetic approach, in which bio-oil components are classified into representative species. Kinetic parameters are derived from experimental data and literature to ensure the accuracy of reaction rates under FCC conditions.

The kinetic model used in this study was developed by [14], who investigated the kinetics of palm oil cracking with a silica-alumina catalyst in a continuous fixed-bed reactor. Three models were proposed to represent the respective cracking reactions over a temperature range of 450–600°C. To achieve a more accurate representation, Model 3 (Figure 2), which describes the catalytic cracking of bio-oil into kerosene, gasoline, and gas plus coke, was selected for this study. Table 2 presents the corresponding pre-exponential factors and activation energies. These values were obtained from a least squares fit conducted by the authors of this study, based on experiments performed by [14].

 doi:10.20944/preprints202506.0674.v1

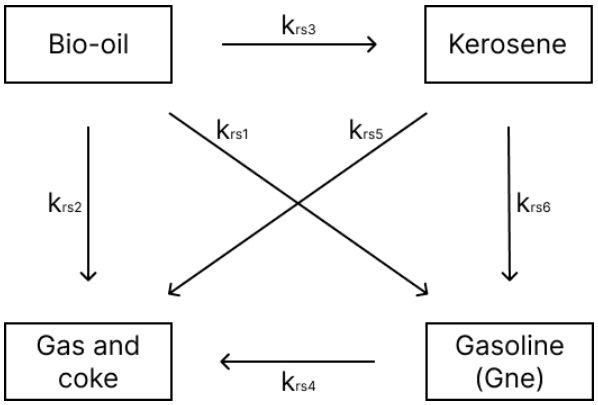

Figure 2. 4-lump bio-oil reaction mechanism.

Table 2. Kinetic data for the 4-lumped bio-oil cracking mechanism from [14].

Reaction number	reactant/product	$k_{r,T}$ ($cm^3/(g_s.min)$)	Activation Energy (kJ/kmol)
1	Bio-oil → Gne	11.359	19,131
2	Bio-oil → Gas + Coke	1.601	2,009
3	Bio-oil → Kerosene	45.271	29,620
4	Gne → Gas + Coke	2.628	13,286
5	Kerosene → Gas + Coke	2.005	25.733
6	Kerosene → Gne	48.634	20,762

Analogous to gas oil kinetics, the pre-exponential factors in Table 2 must be multiplied by the catalyst bulk density to account for the influence of catalyst concentration on reaction rates. This adjustment ensures a more accurate representation of the catalytic cracking process, aligning the bio-oil kinetics with established models for hydrocarbon feedstocks:

$$k_r = k_{r,T} e^{\frac{-E_a}{RT}} \rho_s \epsilon_s. \tag{41}$$

All reactions in the aforementioned mechanism were assumed to follow first-order kinetics. Since certain bio-oil properties are not reported by [14], they were estimated based on the studies conducted by [15,16], ensuring consistency with established methodologies for hydrocarbon processing.

2.3. Numerical sOlution of the Mathematical Model

The set of ordinary differential equations that compose the model was solved by the MATLAB routine ode23s, which can robustly handle stiff systems of ODEs.

3. Results and Discussion

3.1. Model Validation

Model predictions are validated against experimental results from a full-scale FCC riser operating with gas oil, as reported by [10]. The corresponding operating conditions are detailed in Table 3. Key performance indicators, including gas oil conversion and gasoline yield, are examined to evaluate the accuracy of the simulation. However, the droplet diameter distribution is not provided by the authors. To address this limitation, a sensitivity analysis will be conducted to assess its influence on conversion and yield rates, ensuring a comprehensive understanding of its potential impact on reactor performance.

 doi:10.20944/preprints202506.0674.v1

Table 3. Operating conditions for the riser reactor investigated by [10].

Parameter	Value
Inlet pressure	315 kPa
Steam inlet temperature	650 K
Steam mass flowrate	4.25 kg/s
Feed inlet temperature	520 K
Feed flow rate	85 kg/s
CTO	5.5
Catalyst inlet temperature	960 K
Catalyst density	1,500 kg/m^3
Catalyst particle diameter	65 μm

3.1.1. Impact of Heat Transfer Correlations/Mechanisms

Although previous investigations have used fully three-dimensional models ([3]), open questions remain regarding the role of heat transfer mechanisms and correlations. Unlike most prior FCC models, radiation effects have been incorporated into the present work. However, preliminary analyses indicate that radiation is negligible in both the droplet evaporation process and conversion/yield predictions. Since conversion curves with and without radiation effects are nearly identical, they are omitted here for brevity.

Another key aspect worth exploring is the choice of heat transfer correlation. The vast majority of numerical studies on FCC risers, if not all, rely on the Ranz-Marshall correlation (Equation (27)). However, this correlation was originally developed for heat transfer modeling of a single droplet in an unbounded flow, making it well-suited for applications in internal combustion engines and turbines. In FCC risers, additional complexities arise because heat transfer is also influenced by catalyst particles. In this regard, the Buchanan correlation (Equation (28)) provides a more suitable alternative, as it accounts for feed droplet vaporization by considering direct contact, convective heat transfer, and radiative effects during droplet-particle collisions [17].

Figure 3 compares the predicted gas oil conversion and gasoline yield against the experimental results of [10] using the Ranz-Marshall correlation, assuming a droplet diameter of 200 μm. As seen in the figure, the predictions exhibit significant underestimation relative to experimental data.

Figure 4 presents the same numerical setup but using the Buchanan correlation instead. Clearly, agreement with experimental results is notably improved. Figure 5 illustrates the variation in droplet size along the riser height for both heat transfer correlations. As expected, the Buchanan correlation predicts a much faster vaporization rate, which enhances chemical reaction rates.

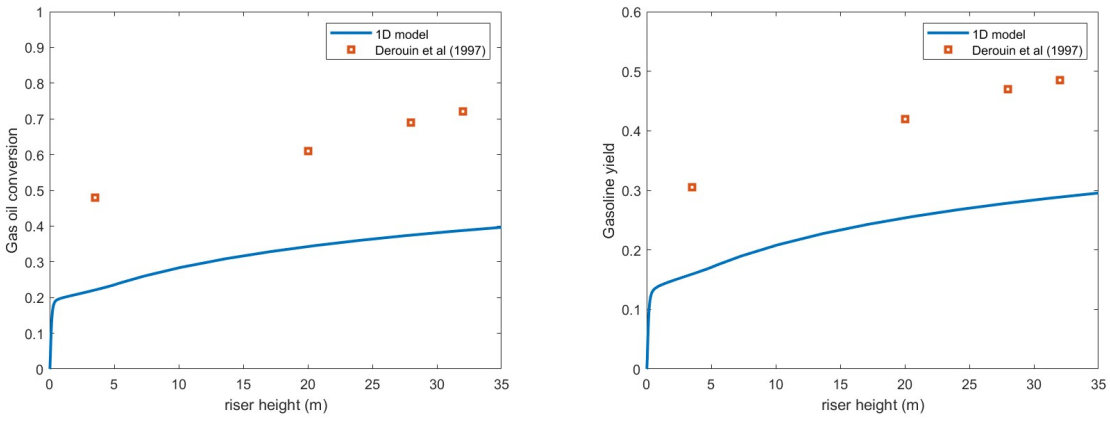

(**a**) (**b**)

Figure 3. (**a**) Gas oil conversion. (**b**) Gasoline yield. Predictions versus experiments using Ranz-Marschall correlation and droplet size = 200 μm.

 doi:10.20944/preprints202506.0674.v1

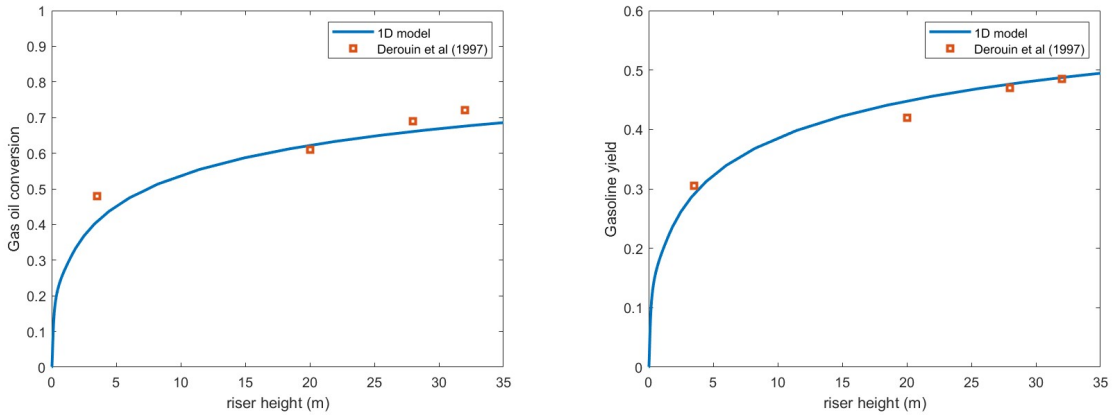

(**a**) (**b**)

Figure 4. (**a**) Gas oil conversion. (**b**) Gasoline yield. Predictions versus experiments using Buchanan correlation and droplet size = 200 μm.

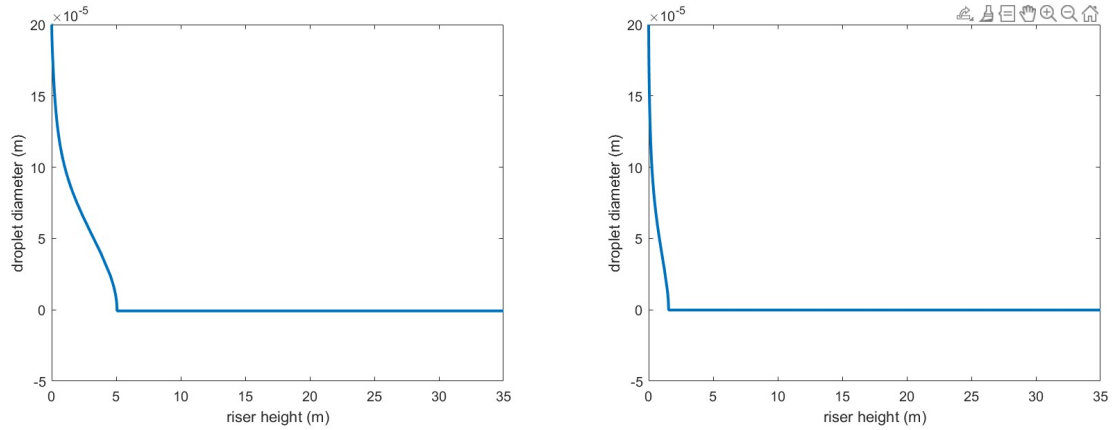

(**a**) (**b**)

Figure 5. (**a**) Droplet size reduction predicted by Ranz-Marschall correlation. (**b**) Droplet size reduction predicted by Buchanan correlation.

Interestingly, several studies that assume fully evaporated feedstock have successfully predicted conversion and yield. These findings suggest that, at least for relatively small droplets, this assumption may be reasonable. However, such models do not account for the impact of droplet size, which remains an important factor in reactor performance predictions.

3.1.2. Impact of Droplet Size

For the analyses presented in this section, the Buchanan model (Equation (28)) was used to calculate heat transfer between the droplets and the gas.

Figures 6 and 7 show the gas oil conversion and gasoline yield for 300 μm and 400 μm droplets, respectively. The results indicate that droplet size significantly affects reaction rates, primarily because rapid feed vaporization is crucial for process efficiency.

 doi:10.20944/preprints202506.0674.v1

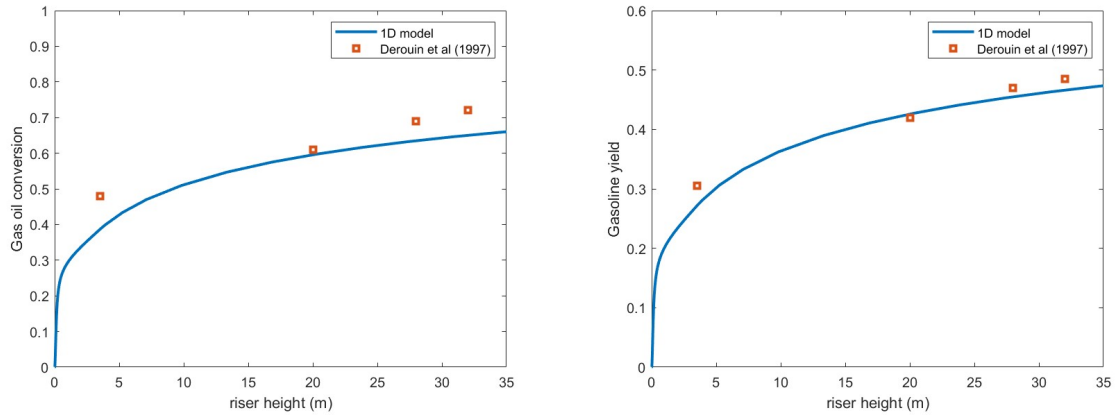

(**a**) (**b**)

Figure 6. (**a**) Gas oil conversion. (**b**) Gasoline yield. Predictions versus experiments using Buchanan correlation and droplet size = 300 μm.

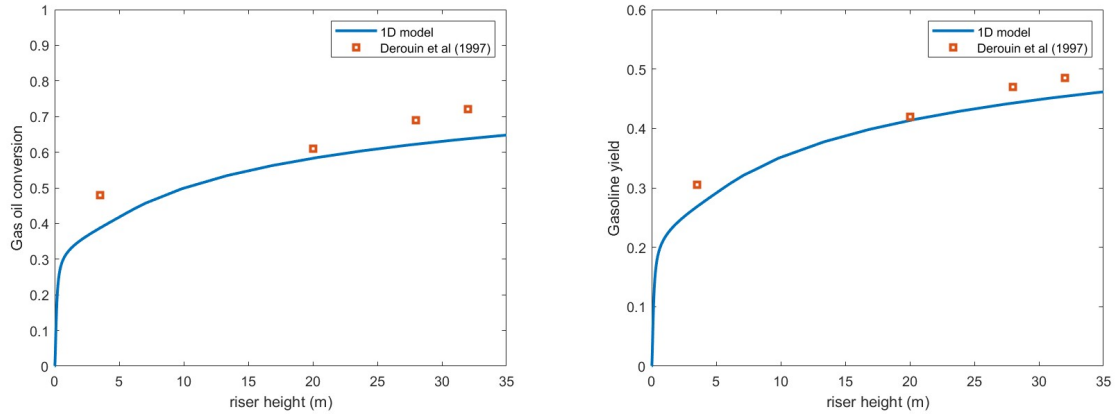

(**a**) (**b**)

Figure 7. (**a**) Gas oil conversion. (**b**) Gasoline yield. Predictions versus experiments using Buchanan correlation and droplet size = 400 μm.

3.2. Bio-Oil Simulation

To analyze the impact of operating conditions identical to those in the gas oil simulations, bio-oil catalytic cracking conversion and yield rates were initially investigated under the conditions specified in Table 3, with 200-μm-diameter droplets injected.

Figure 8 presents bio-oil conversion and yield for gas and coke, gasoline and kerosene, and droplet diameter in a 35-m riser operating under the defined conditions. As observed, bio-oil conversion is substantially lower than that of gas oil under the same conditions (Figure 4), and the droplets only partially vaporize. Furthermore, the vaporization process occurs at a significantly slower rate compared to gas oil droplets, Figure 5.

Although the vaporized bio-oil mass accounts for approximately 65.7 % of the injected feed, it is important to note that the calculated conversion/yield considers only the bio-oil in the gas phase. Consequently, the actual conversion to other products remains highly inefficient under these operating conditions.

These results can be partly explained by the bio-oil's latent heat of vaporization, which is nearly an order of magnitude higher than that of gas oil (Table A1). Above approximately 10 meters, the three phases—oil, gas, and catalyst particles—reach thermal equilibrium at the bio-oil boiling point, meaning a substantially higher energy input is required for complete feed vaporization. Reducing droplet size enhances heat transfer but does not significantly improve vaporization, as no additional

 doi:10.20944/preprints202506.0674.v1

energy is supplied to the reactor. Indeed, a further reduction in droplet diameter to 50 μm still resulted in incomplete feed vaporization and no significant improvements in conversion or yield.

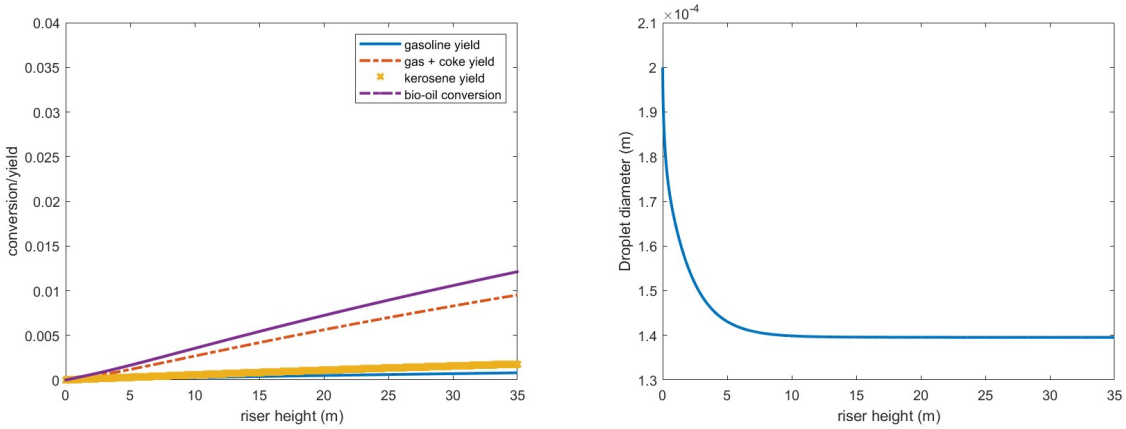

(**a**) (**b**)

Figure 8. (**a**) Bio-oil conversion and product yield in the operating conditions indicated in Table 3. (**b**) Bio-oil droplet diameter.

To explore potential performance enhancements, the catalyst-to-oil ratio (CTO) was increased to 7 while maintaining the steam and feed flow rates. Results, shown in Figure 9, indicate no improvement in conversion and yield, although more of the feed vaporizes, approximately 78 %. Vaporization is even slower than the previous case, therefore consuming energy for the chemical reactions to occur efficiently.

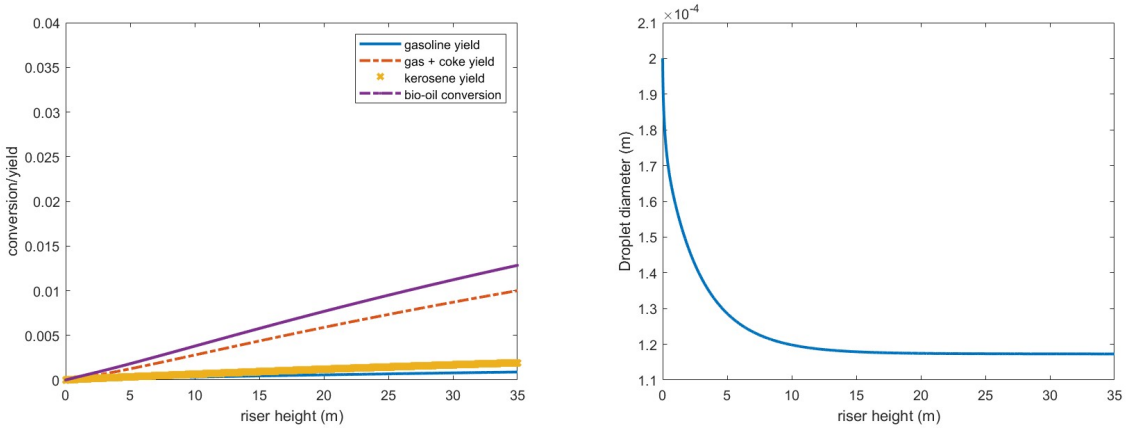

(**a**) (**b**)

Figure 9. (**a**) Bio-oil conversion and product yield in the operating conditions indicated in Table 3 but CTO=7. (**b**) Bio-oil droplet diameter.

Figure 10 presents results obtained by doubling the steam flow rate while maintaining the other parameters from Table 3. Despite the increased energy input, conversion and yield decrease. This seemingly counterintuitive outcome is attributed to the higher gas velocity and poor vaporization rate, which reduces residence time and slows droplet vaporization. These findings indicate that the kinetics of bio-oil on the investigated catalyst is significantly slower than that of gas oil. While droplet vaporization has been observed to be incomplete under the conditions studied so far, the rate of chemical reactions remains the limiting step in the overall catalytic conversion process. Indeed, the one-dimensional solution does not consider some flow particularities as the core-annulus solid distribution and back-mixing that can modify the reaction dynamics. However, Ranganathan and Gu

 doi:10.20944/preprints202506.0674.v1

(2018) also observed very low yield when simulating the catalytic cracking of pyrolysis vapors in a pilot-scale FCC riser using CFD.

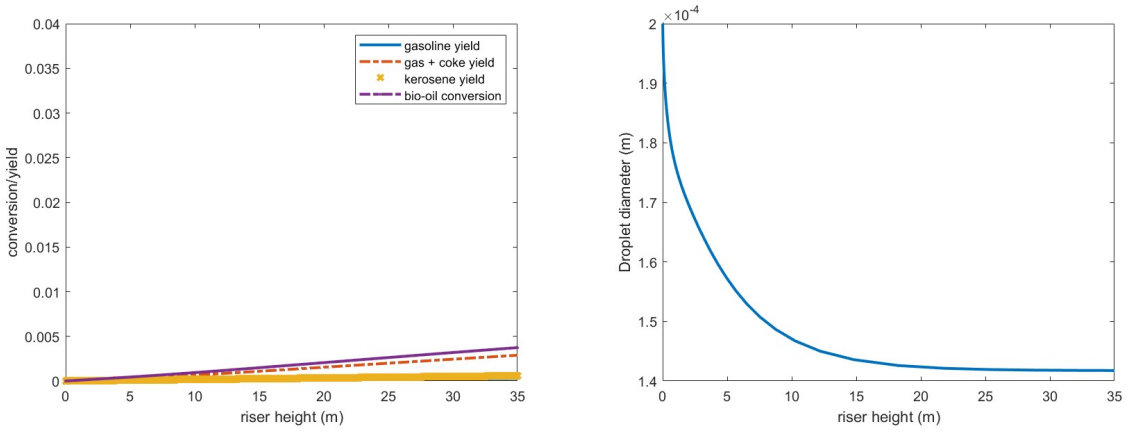

(**a**) (**b**)

Figure 10. (**a**) Bio-oil conversion and product yield in the operating conditions indicated in Table 3 but steam flow rate is 8.5 kg/s. (**b**) Bio-oil droplet diameter.

Another critical consideration in bio-oil processing is the maximum allowable steam and catalyst temperatures, as excessive heat can degrade the feedstock. While this aspect lies beyond the scope of the present study, such thermal limits represent additional constraints for efficient bio-oil FCC processing. No attempts were made to modify these parameters.

Given the inefficiency of bio-oil vaporization, the challenges of effectively increasing heat input, and the slow chemical kinetics involved, one potential strategy to enhance conversion and yield is to reduce the feed flow rate.

Figure 11 illustrates the results of processing an oil flow rate equivalent to 10% of the gas oil, while maintaining all other parameters as originally derived from Table 3.

Vaporization is now significantly more efficient, with complete vaporization occurring within 5 meters above injection. However, despite some improvement compared to previous cases, conversion and yield remain quite low. Since feed vaporization is no longer the bottleneck in the cracking process, the observed conversion and yield must be influenced by other operating conditions, such as catalyst and steam inlet temperature. These test cases underscore the inherent challenges of processing biofuels with vaporization properties and chemical reaction mechanisms that differ significantly from those of gas oil within current FCC operating ranges.

Another important finding is that, across all analyzed scenarios, the primary products were coke and gas, aligning with the results reported by [14]. Catalyst deactivation was negligible, as coke formation remained insignificant.

In conclusion, these analyses highlight the usefulness of the reduced-order model in identifying challenges associated with adapting existing FCC facilities for bio-oil processing. The simplified yet representative mathematical framework provides rapid insights into fundamental bottlenecks, reinforcing the need for further research into FCC riser performance when handling gas oil/bio-oil blends.

 doi:10.20944/preprints202506.0674.v1

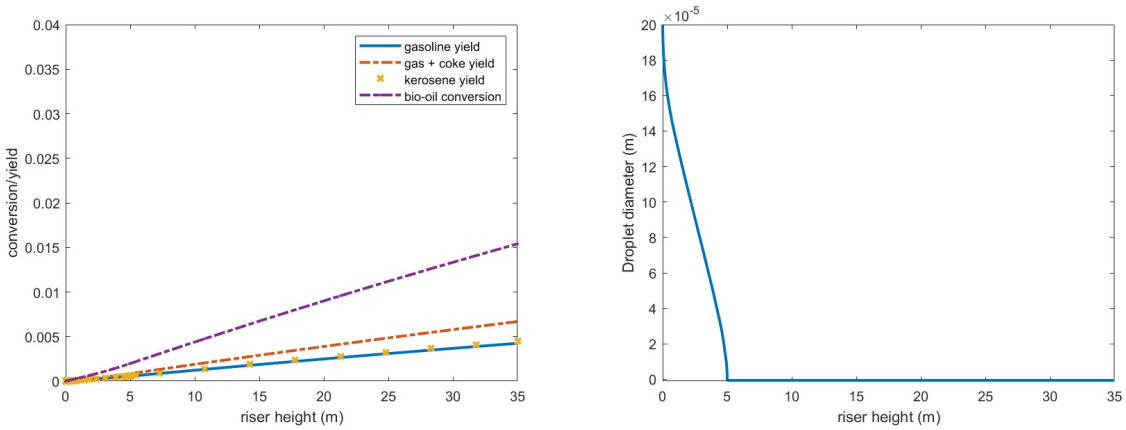

(**a**) (**b**)

Figure 11. (**a**) Bio-oil conversion and product yield in the operating conditions indicated in Table 3 but feed flow rate is 8.5 kg/s. (**b**) Bio-oil droplet diameter.

4. Conclusions

A reduced-order model for simulating FCC risers operating with bio-oil is introduced, enabling a rapid assessment of reactor performance under such conditions. The main conclusions of this study can be summarized as follows:

- Thermal radiation effects on droplet evaporation, and consequently on reactor performance, are negligible under the investigated operating conditions;
- The Ranz-Marschall correlation underestimates droplet vaporization, leading to an underprediction of conversion and yield. In contrast, the Buchanan correlation provides a more accurate representation of the complex heat transfer mechanisms within FCC risers;
- The vaporization heat of palm bio-oil requires significantly higher heat input for complete vaporization compared to gas oil under identical operating conditions. This is due to its vaporization heat being nearly an order of magnitude greater than that of gas oil;
- FCC reactor performance is largely insensitive to bio-oil droplet diameter, primarily as a natural consequence of its substantially higher vaporization heat and slow chemical kinetics;
- Optimal operating conditions for processing bio-oil—i.e., maximizing the production of higher-value products—differ from conventional gas oil conditions. Indeed, most decarbonization efforts in the oil industry focus on processing blends of bio-oils and gas oil, rather than pure bio-oil;
- The proposed model can be effectively utilized to optimize FCC units operating with biofuels and bio-oil/gas oil blends, provided that the necessary cracking kinetics data is available.

It is important to emphasize that this model, like other models based on transport and conservation equations, relies heavily on accurate physical and chemical property data. Future research should prioritize precise measurements, particularly given the wide variations in bio-oil composition.

Author Contributions: Conceptualization, F.S, J.U., G.N., A.R., H. R. and H.M.; methodology, F.S, J.U., G.N., A.R., H. R. and H.M.; software, F.S, J.U., G.N., A.R., H. R. and H.M.; validation, F.S, J.U., G.N., A.R., H. R. and H.M.; formal analysis, F.S, J.U., G.N., A.R., H. R. and H.M.; investigation, F.S, J.U., G.N., A.R., H. R. and H.M.; resources, F.S, J.U., G.N., A.R., H. R. and H.M.; data curation, F.S, J.U., G.N., A.R., H. R. and H.M.; writing—original draft preparation, F.S, J.U., G.N., A.R., H. R. and H.M.; writing—review and editing, F.S, J.U., G.N., A.R., H. R. and H.M.; visualization, F.S, J.U., G.N., A.R., H. R. and H.M.; supervision, F.S, J.U., G.N., A.R., H. R. and H.M.; project administration, J.U.; funding acquisition, J.U. and H.M. All authors have read and agreed to the published version of the manuscript.

Funding: This research was funded by Petrobras Project BIOMIST+RESIDMIST (cooperation term 0050.0127779.24.9), CAPES and CNPq.

 doi:10.20944/preprints202506.0674.v1

Conflicts of Interest: The authors declare no conflicts of interest.

Appendix A

Appendix A.1

Here we provide the physical/transport properties adopted in the model for repeatability purposes.

Table A1. Physical properties of species.

Property	Value
Gas heat capacity	2 kJ/(kg.K)
Solid density	1,500 kg/m^3
Solid heat capacity	1.090 kJ/(kg.K)
Gas oil molecular weight	371 kg/kmol
Gas oil vaporizing temperature	530 K
Gas oil boiling point	560 K
Gas oil vaporization latent heat	250 kJ/kg
Gas oil density	925.9 kg/m^3
Gas oil diffusion coefficient	3.79x10$^{-6}m^2/s$
Gas dynamic viscosity	1.72x10^{-5} $kg/(m.s)$
Gas thermal conductivity	0.045 W/(m.K)
Emissivity	0.9
Gasoline molecular weight	106 kg/kmol
Kerosene molecular weight	170 kg/kmol
Light gas molecular weight	40 kg/kmol
Coke molecular weight	371 kg/kmol
Bio-oil molecular weight	810 kg/kmol
Bio-oil vaporizing temperature	530 K
Bio-oil boiling point	560 K
Bio-oil vaporization latent heat	2760 kJ/kg
Bio-oil density	800 kg/m^3
Bio-oil diffusion coefficient	3.79x10$^{-6}m^2/s$

References

1. Pinho, A.R.; Almeida, M.B.; Mendes, F.L.; Casavechia, L.C.; Talmadge, M.S.; Kinchin, C.M.; Chum, H.L. Fast pyrolysis oil from pinewood chips co-processing with vacuum gas oil in an FCC unit for second generation fuel production. *Fuel* **2017**, *188*, 462–473.
2. Eschenbacher, A.; Myrstad, T.; Bech, N.; Duusd, J.Ø.; Li, C.; Jensen, P.A.; Henriksen, U.B.; Ahrenfeldt, J.; Mentzel, U.V.; Jensen, A.D. Co-processing of wood and wheat straw derived pyrolysis oils with FCC feed—Product distribution and effect of deoxygenation. *Fuel* **2020**, *260*, 116312.
3. Lopes, G.; Rosa, L.; Mori, M.; Nunhez, J.; Martignoni, W. Three-dimensional modeling of fluid catalytic cracking industrial riser flow and reactions. *Computers & Chemical Engineering* **2011**, *35*, 2159–2168. https://doi.org/https://doi.org/10.1016/j.compchemeng.2010.12.014.
4. Nayak, S.V.; Joshi, S.L.; Ranade, V.V. Modeling of vaporization and cracking of liquid oil injected in a gas–solid riser. *Chemical Engineering Science* **2005**, *60*, 6049–6066. 7th International Conference on Gas-Liquid and Gas-Liquid-Solid Reactor Engineering, https://doi.org/https://doi.org/10.1016/j.ces.2005.04.046.
5. Al-Sabawi, M.; Chen, J.; Ng, S. Fluid Catalytic Cracking of Biomass-Derived Oils and Their Blends with Petroleum Feedstocks: A Review. *Energy & Fuels* **2012**, *26*, 5355–5372, [https://doi.org/10.1021/ef3006417]. https://doi.org/10.1021/ef3006417.
6. Ranganathan, P.; Gu, S. Numerical simulation of catalytic upgrading of biomass pyrolysis vapours in a FCC riser. *Fuel Processing Technology* **2018**, *171*, 162–172. https://doi.org/https://doi.org/10.1016/j.fuproc.2017.11.008.
7. Brenner, T.A.; Fontenot, R.L.; Cizmas, P.G.; O'Brien, T.J.; Breault, R.W. A reduced-order model for heat transfer in multiphase flow and practical aspects of the proper orthogonal decomposition. *Computers & Chemical Engineering* **2012**, *43*, 68–80.

 doi:10.20944/preprints202506.0674.v1

8. Huang, C.; Duraisamy, K.; Merkle, C. Challenges in reduced order modeling of reacting flows. In Proceedings of the 2018 Joint Propulsion Conference, 2018, p. 4675.
9. Selalame, T.W.; Patel, R.; Mujtaba, I.M.; John, Y.M. The Effects of Vaporisation Models on the FCC Riser Reactor. *Energies* **2023**, *16*. https://doi.org/10.3390/en16124831.
10. Derouin, C.; Nevicato, D.; Forissier, M.; Wild, G.; Bernard, J.R. Hydrodynamics of Riser Units and Their Impact on FCC Operation. *Industrial & Engineering Chemistry Research* **1997**, *36*, 4504–4515, [https://doi.org/10.1021/ie970432r]. https://doi.org/10.1021/ie970432r.
11. Schiller, L.; Naumann, A. A Drag Coefficient Correlation. *Zeitschrift des Vereins Deutscher Ingenieure* **1935**, *77*, 318–320.
12. Farag, H.; Blasetti, A.; de Lasa, H. Catalytic Cracking with FCCT Loaded with Tin Metal Traps. Adsorption Constants for Gas Oil, Gasoline and Light Gases. *Industrial & Engineering Chemistry Research* **1994**, *33*, 3131–3140, [https://doi.org/10.1021/ie00036a031]. https://doi.org/10.1021/ie00036a031.
13. Han, I.S.; Chung, C.B. Dynamic modeling and simulation of a fluidized catalytic cracking process. Part II: Property estimation and simulation. *Chemical Engineering Science* **2001**, *56*, 1973–1990. https://doi.org/https://doi.org/10.1016/S0009-2509(00)00494-2.
14. Sunarno, S., R.R.M.P.A.M.; Budiman, A. Kinetic study of catalytic cracking of bio-oil over silica-alumina catalyst. *BioResources* **2018**, *13*, 1917–1929, https://doi.org/10.15376/biores.13.1.191701929.
15. Terrell, E. Estimation of Fuel Properties for the Heavy Fraction of Biomass Pyrolysis Oil Consisting of Proposed Structures for Pyrolytic Lignin and Humins. *Energies* **2024**, *17*. https://doi.org/10.3390/en17092011.
16. Chempro., [https://chempro.in/palmoilproperties.htm].
17. Buchanan, J.S. Analysis of heating and vaporization of feed droplets in fluidized catalytic cracking risers. *Industrial and Engineering Chemistry Research; (United States)* **1994**, *33:12*. https://doi.org/10.1021/ie00036a027.